Branching of Colloidal Chains in Capillary-Confined Nematics

Pavel Kossyrev,[1,*,†] Miha Ravnik,[2] and Slobodan Žumer[2,3]

[1]*Department of Materials Science and Engineering, Massachusetts Institute of Technology, 77 Massachusetts Avenue, NE47-4th floor, Cambridge, Massachusetts 02139, USA*

[2]*Department of Physics, University of Ljubljana, Jadranska 19, 1000 Ljubljana, Slovenia*

[3]*J. Stefan Institute, Jamova 39, 1000 Ljubljana, Slovenia*

(Received 6 May 2005; published 2 February 2006)

We report on the observation of colloidal chain assembly and branching inside capillaries filled with a nematic liquid crystal. Because of the homeotropic anchoring of liquid crystalline molecules on the capillary and colloidal droplet surfaces, the assembly of droplets along the capillary axis is expected, producing a transformation of the nematic director field from an escape-radial to quasiradial configuration. However, the subsequent over time branching of the straight colloidal chains is counterintuitive. By numerical simulations, we demonstrate that chain branching can occur by overcoming an energy barrier and can at least dwell as a metastable configuration. Moreover, manipulation of colloidal chains by electric fields and their gradients demonstrates various regimes of chain behavior in electric fields.

DOI: 10.1103/PhysRevLett.96.048301 PACS numbers: 82.70.−y, 61.30.Dk, 61.30.Pq

A previously reported new class of colloidal interactions can arise in emulsions of isotropic fluids that form droplets in the host of nematic liquid crystals (LCs) [1]. These interactions may govern the microdroplets of isotropic fluid to assemble into chains. Originally, chains of water droplets were observed inside large droplets of nematics [1]. When emulsions of LC and polymer were produced inside a planar cell, the chains of polymer droplets formed ordered arrays [2]. Recently, one- and two-dimensional (1D, 2D) droplet structures were observed at the LC-air interfaces [3]. In the above examples, the delicate balance between colloidal interactions in anisotropic fluids govern the assembly of regular 1D and 2D arrays of droplets. A regular structure that exhibits a structural instability is an interesting test ground for studying the details of colloidal interactions. In this Letter, we demonstrate that emulsions of polymer droplets in the host of LC, which are confined inside cylindrical capillaries, assemble along the capillary axis transforming the LC director field from an escape-radial to quasiradial configuration. Surprisingly, branching of the initially straight chains of droplets is observed over time. We investigate this branching instability by numerical simulations based on the Frank elasticity. Moreover, we report on the manipulation of droplet chains by external electric fields, and show that the dielectric interactions within an inhomogeneous electric field are crucial for chain manipulation.

In general, the cylindrical geometry has attracted many studies of the properties of confined LC and the distribution of LC molecular orientations, described by a spatially varying unit vector called the director [4,5]. For example, polarizing optical microscopy of the birefringence of the escape-radial molecular configuration can reveal the elastic constants and anchoring energy on capillary walls for nematics [5]. The escape-radial configuration that appears when molecules are anchored perpendicularly to capillary walls is observed for almost all practical capillaries, such as the capillary radius $R > 20l \approx 40$ nm, where $l \approx 2$ nm is a common molecular length of low-molecular-weight nematics [6]. We stabilized the escape-radial configuration inside a 50 μm diameter cylindrical capillary by treating the inner capillary walls with a lecithin surfactant to enforce homeotropic (perpendicular to surface) anchoring [7]. As shown in Fig. 1(a), the regions along the capillary axis that do not include polymer droplets possess the escape-radial configuration, the characteristic birefringence of which displays symmetrical light and dark bands parallel to the capillary axis that reverse upon 45° rotation of cross polarizers.

To prepare chains of droplets situated on the capillary axis, we filled the capillaries with a homogeneous mixture of pentylcyanobiphenyl (5CB) LC containing 1 wt. % of polydimethyl-siloxane (PDMS) polymer at elevated temperatures of 50 °C. Upon cooling to room temperature, the polymer phase separates from the LC to form droplets.

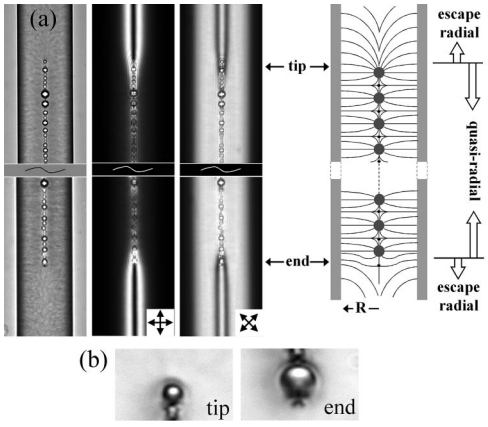

FIG. 1. (a) Microscope images of the structure in white light and between cross polarizers. The directions of polarizers are indicated. (b) The tip and the end of a droplet chain showing that the companion defects are positioned under the droplets.

Below 35 °C, the clearing point of 5CB, which possesses a nematic phase between 23–35 °C, the droplets merge into the center of the capillary. The axial droplet position is preferred due to homeotropic anchoring of 5CB molecules on PDMS droplet surfaces [7], producing the least elastic distortions to the nematic host. Over time, single droplets migrate along the capillary axis to assemble into chains. The droplet diameter within a chain can be predicted [2] by balancing the energies of anchoring, wa^2, and elastic distortions Ka of LC host around a droplet. Measured by optical means the droplet diameter $a \approx 3$ μm is in satisfactory agreement with this energy balance assumption, where the surface energy for cyanobiphenyl LC and silicon-based materials, $w = 5 \times 10^{-6}$ J/m^2, and the elastic constant of LC in one constant approximation, $K = 10^{-11}$ N, were used from the literature [6,8].

Long-range attractive and short-range repulsive interactions between droplets arising from the orientational elastic energy of nematic LC host can be the reason for the formation of colloidal chains [1]. A droplet with homeotropic anchoring for LC molecules that is introduced into the capillary with an escape-radial LC configuration forces the LC to produce a defect. This companion defect is situated on the capillary axis in the droplet vicinity, where the distance between the defect and droplet center scales linearly with the droplet diameter [1]. As shown in Fig. 1(b), the escape-radial LC configuration promotes companion defects to form under droplets, when going from the tip to the end of droplet chains. A droplet-defect pair, akin to an electrostatic dipole, attracts a similar pair that can be rather well described by an effective long-range dipole-dipole potential:

$$U_{ij} = K p_i p_j \frac{1 - 3\cos^2\theta}{r^3}, \qquad (1)$$

where θ and r are the angle and the distance, respectively, between the interacting dipoles p_i and p_j. On a short scale, the presence of a topological defect between two droplets induces droplet repulsion inhibiting their coalescence. Some droplet coalescence, however, can be observed as a result of chain metastability [see Fig. 1(a)].

Assembled chains produce significant perturbation to the escape-radial LC configuration. For long chains of droplets the perturbation transforms the escape-radial configuration into a quasiradial configuration [see Fig. 1(a)]. By observing the formation of chains, we evaluated that approximately 5–10 droplets are necessary to produce significant perturbation resulting in the quasiradial LC configuration, the dark field of which switches to bright upon 45° rotation of cross polarizers, as shown in Fig. 1(a).

A chain of droplets in a nematic host is metastable rather than in equilibrium. One of the interesting phenomena that can appear as a result of metastability is the formation of side branches perpendicular to the capillary axis (see Fig. 2). The observed branching can constitute of one or more droplets off the straight axial chains.

To determine whether branching is favorable, one must go beyond the effective dipole-dipole potential, Eq. (1), which only predicts the formation of straight droplet chains. We performed numerical simulations to compute and compare the elastic free energy of the nematic LC for a straight colloidal chain and a chain with an additional off-chain droplet. The director field for both configurations was calculated in the equal elastic constant approximation [6] with the infinite homeotropic anchoring on all surfaces by minimization of the Frank free energy F:

$$F = \frac{1}{2} K \int_{\mathrm{LC}} [(\mathrm{div}\mathbf{n})^2 + (\mathrm{curl}\mathbf{n})^2] dV, \qquad (2)$$

where K is the elastic constant, $\mathbf{n}$ is the nematic director, and the integration is performed over the whole volume of LC with a resolution for director smaller than 0.1 μm. For our simulations we took the droplet diameter $a = 3$ μm, capillary radius $R = 20$ μm, and LC elastic constant $K = 10^{-11}$ N. The Euler–Lagrange equations obtained from the minimization of Eq. (2), were discretized by a finite difference method on a cubic mesh and then solved by an explicit relaxation method algorithm [9]. For the mesh resolution of 0.1 μm, about 3×10^4 iterations were needed to yield better than ~1% convergence of the free energy. The hyperbolical defects positioned at (x_d^k, y_d^k, z_d^k) were described by the analytical ansatz $[x - x_d^k, y - y_d^k, -(z - z_d^k)]/\sqrt{(x - x_d^k)^2 + (y - y_d^k)^2 + (z - z_d^k)^2}$, where k stands for each defect, and x, y, and z are the Cartesian coordinates [10]. This ansatz was used in the Euler–Lagrange equations to determine the director condition in the nearest lattice points surrounding each defect.

The droplet-droplet distance in the chain and off-chain positions are the two major parameters that characterize the colloidal structure. By numerical minimization, we obtained for both parameters an equilibrium value $d = (1.26 \pm 0.07)a$ [see Figs. 3(a) and 3(b)] that agrees with our experimental results (see Fig. 2). This droplet-

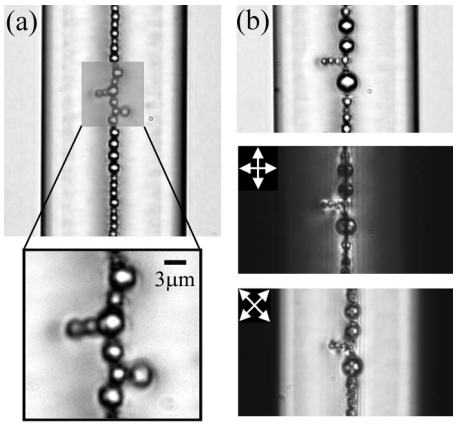

FIG. 2. (a) A chain with two close branches. Branching of chains is observed after an equilibration time of ~1 week. (b) A region of branched chain in white light and between cross polarizers. The directions of polarizers are indicated.

droplet distance is slightly higher (by ≈8%) then the one predicted in Ref. [1], but we should stress that, contrary to Ref. [1], in our calculations no multipole ansatz functions were used.

Note that in order to fairly compare the elastic free energies of straight and branched chain configurations the LC volume and the number of considered droplets must be the same for both configurations. Therefore, we compared a segment of a total of 5 axial droplets [see inset of Fig. 3(a)] with a segment of 4 axial plus 1 off-chain droplet accompanied with a $1.26a$ long segment of pure escape-radial structure as needed to maintain equal LC volumes [see inset of Fig. 3(b)]. Our results show that the total elastic free energy F of the straight 5 droplet segment exhibits a quadratic dependence on the lateral displacement of one of the middle droplets with a global minimum $\approx 2.158 \times 10^{-15}$ J [see Fig. 3(a)]. This value is only slightly lower than the local minimum of the free energy of the chain with an off-chain droplet, $\approx 2.271 \times 10^{-15}$ J [see Fig. 3(b)]. Within our equal elastic constant approximation the straight configuration is the equilibrium one separated by an energy barrier from the metastable structure, described by one droplet in the off-chain position. The small difference in the calculated free energies for the two configurations indicates that considering nonequal Frank elastic constants and possible heterogeneity of droplet sizes may easily yield more comparable energy minima or may even reverse their stability. Indeed, our additional numerical calculations indicate that the heterogeneity of droplet sizes relevant to our system can further reduce the difference between the free energy minima of straight and branched configurations by ~30%.

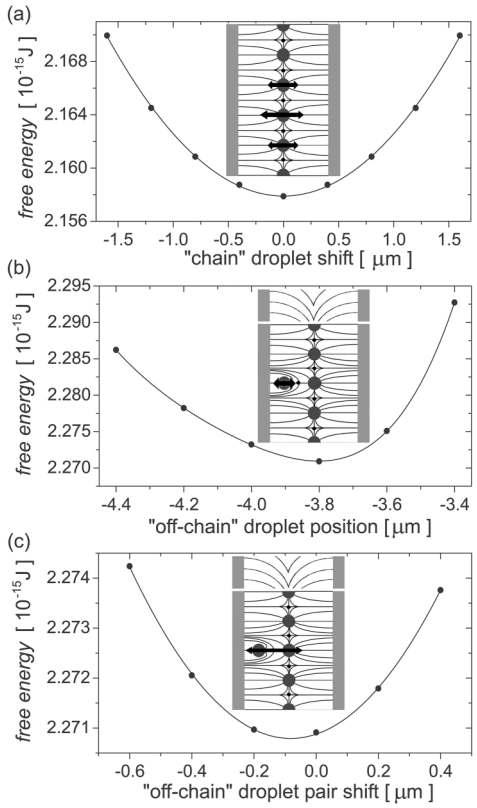

FIG. 3. Numerical results. Free energy is determined within ±5% precision. (a) The elastic free energy F of a straight 5 droplet segment as a function of lateral shift of one of the middle droplets. Note that the central droplet (large arrow), upper and lower neighbor droplets (small arrows), and all 4 neighbor defects were shifted at the same time. When the central droplet was shifted, for example, by 4 units, the upper (lower) neighbor defect was shifted by 3 units, the upper (lower) neighbor droplet by two units, and upper (lower) second-neighbor defect by one unit. (b) Dependence of F for a branched 5 droplet configuration on the radial position of off-chain droplet. To satisfy the equal volume requirement, an escaped-radial elastic free energy $F_{\mathrm{esc}} = 3\pi K d$ was added to F. (c) Elastic free energy as a function of the chain and off-chain droplet pair shift in radial direction. The distance d between the chain and off-chain droplets was fixed. Analogous to (b), F_{esc} was added.

We could speculate on the origin of off-chain droplet formation. When the escape-radial structure is ''energy expensive'' in comparison with the colloidal chain configuration, the formation of long straight chains is favorable. On the contrary, when the escape-radial structure is ''inexpensive'' (e.g., $a \ll 2R$), a colloidal chain prefers to be as short as possible to maximize the escaped director volume, and droplets can be pushed out of capillary axis. In our system the escaped structure is neither expensive nor inexpensive resulting in very close values for the elastic energy of the straight and branched chains.

Our numerical results also explain a slight bending of axial colloidal chains at places where off-chain droplets are present [see Fig. 2(a)]. We have shifted a chain and its neighboring off-chain droplets in the radial direction and calculated the elastic free energy [see Fig. 3(c)]. A minimum is obtained at distance ≈ -0.1 μm from the capillary axis, which is very close to the experimental observations. The chain bending can be qualitatively understood by the mechanism of ''elastic repulsion'' between the off-chain droplet and its 2 second closest neighbors. Indeed, the director field is unable to relax smoothly if it is too strongly confined by droplet surfaces, and, therefore, pushes the chain and off-chain droplet pair slightly in the radial direction.

Interestingly, when we modify the LC configuration by an external electric field oriented perpendicular to the capillary axis, chains display cooperative motion without disassembling into single droplets or shorter chains. We observe different electric field regimes of chain behavior affiliated with an appearance of up to two disclination line (DL) pairs of $\pm 1/2$ strength or their absence (zero DL regime). The formation of DLs, monitored by a polarizing microscope, occurs in the axial capillary plane that is perpendicular to the direction of electric field. When one or no DL pairs are formed, the chain motion is to the capillary walls with a typical speed of a few μm/s (see Fig. 4). In most cases, the chain motion happens in the zero DL regime, as expected due to the energy barrier to form a

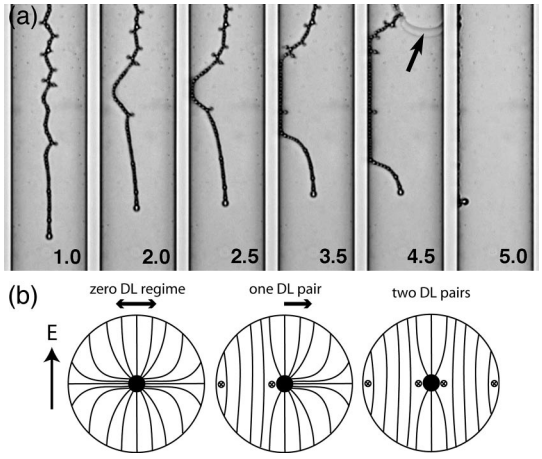

FIG. 4. (a) Most commonly observed droplet chain behavior in electric field (2 V/μm), which is perpendicular to the plane of observation. The time elapsed from the beginning of field application is indicated in seconds. The front shown by an arrow propagating down the capillary corresponds to the transition from the zero DL regime at earlier time to a DL regime at later time. Note that this transition happens at least 10 times faster than the chain movement in earlier time frames. (b) Cross-sectional view of different regimes of chain motion. Filled circle represents a chain, small circles represent $\pm 1/2$ DLs, and LC director orientation is shown by solid lines. The direction of chain motion is indicated by arrows.

DL. Indeed, for a typical nematic, the energy per unit length of a $\pm 1/2$ DL is $\sim 10^{-10}$ J/m [10]. However, when two DL pairs are formed, one on each side of a chain, the chain stays fixed in the central axial position.

These observations can be explained by the appearance of forces on colloidal droplets due to an inhomogeneous electric field [11] and LC elasticity, which is coupled with the electric field as a result of the dielectric anisotropy of LC [6]. In an experiment at micrometer scale one cannot completely avoid inhomogeneities in the electric field caused mainly by the small tilt between electrode plates, resulting in a gradient force on immersed droplets. In our experiment the tilt angle can be at most $\sim \pm 3°$, producing a gradient force of ~ 5 pN per droplet in the direction to capillary walls [12]. This gradient force can be unidirectional or opposite to the "LC force" that acts on the colloidal droplets due to LC distribution in inhomogeneous electric field. From our numerical calculations for the zero DL regime, we obtained the LC force 5–10 pN, which points to capillary axis [13]. Thus, in the zero DL regime, a competition between the gradient and LC forces occurs, which can result in a motion of colloidal chains towards capillary walls. However, for the regime of two DL pairs, each on opposite sides of the chain, we obtain the LC force that is at least an order of magnitude larger. If two DL pairs form before the chain relocation to capillary walls, the LC force is much stronger, and, no matter the gradient force, the chain is stabilized in the central axial position.

In summary, we have demonstrated colloidal assembly in supramicrometer capillaries that produces a transformation of LC director from escape-radial to quasiradial configuration. Not predicted by standard theory, branching of initially straight colloidal chains was observed and discussed in terms of deformational free energy of the LC director field. The analysis indicates that the off-chain droplet configuration is possible but metastable within the one elastic constant approximation. Experimental and numerical results on colloidal chains in external electric fields point out that colloidal structures can be easily manipulated by controlling the electric field and its gradient. Geared towards obtaining stabilized and structured colloids in various geometries and creating a pathway to new materials with potentially useful applications, we hope that this report will generate further investigations of these fascinating systems, where the detailed understanding of interactions plays a crucial role.

P. K. acknowledges Robert Pelcovits for helpful discussions and the support of the U.S. Army through the Institute for Soldier Nanotechnologies, under contract No. DAAD-19-02-D-0002 with the U.S. Army Research Office. M. R. and S. Z. acknowledge financial support by the Slovenian Research Agency (Programme P1-0099 and Slo-US Project Nos. 04-05/32 and NSF 0306851).

*Current Address: Division of Engineering, Brown University, 182 Hope St., Box D, Providence, RI 02912, USA.
†Corresponding author.
Electronic address: Pavel_Kossyrev@brown.edu

[1] P. Poulin, H. Stark, T. C. Lubensky, and D. A. Weitz, Science **275**, 1770 (1997).
[2] J.-C. Loudet, P. Barois, and P. Poulin, Nature (London) **407**, 611 (2000).
[3] I. I. Smalyukh *et al.*, Phys. Rev. Lett. **93**, 117801 (2004).
[4] C. Williams, P. Pieranski, and P. E. Cladis, Phys. Rev. Lett. **29**, 90 (1972).
[5] R. D. Polak, G. P. Crawford, B. C. Kostival, J. W. Doane, and S. Zumer, Phys. Rev. E **49**, R978 (1994).
[6] P. G. de Gennes and J. Prost, *The Physics of Liquid Crystals* (Oxford University Press, New York, 1993).
[7] J. Cognard, Mol. Cryst. Liq. Cryst. Suppl. **1**, 1 (1982).
[8] O. D. Lavrentovich, V. G. Nazarenko, V. V. Sergan, and G. Durand, Phys. Rev. A **45**, R6969 (1992).
[9] W. H. Press, B. P. Flannery, S. A. Teukolsky, and W. T. Vetterling, *Numerical Recipes* (Cambridge University Press, Cambridge, England, 1986).
[10] M. Kleman and O. Lavrentovich, *Soft Matter Physics* (Springer-Verlag, New York, 2003).
[11] T. Jones, *Electromechanics of Particles* (Cambridge University Press, Cambridge, England, 1992).
[12] The force was evaluated following the formalism of [11]. We used the outer capillary diameter 80 μm for the cell gap and the PDMS dielectric constant of 2.5.
[13] We have performed extensive numerical calculations minimizing $F = \frac{1}{2} K \int_{\mathrm{LC}} [(\mathrm{div}\mathbf{n})^2 + (\mathrm{curl}\mathbf{n})^2] dV - \frac{1}{2} \epsilon_0 \epsilon_a \times \int (\mathbf{n} \cdot \mathbf{E})^2 dV$, where $\epsilon_a = 20.1$ is dielectric anisotropy of 5CB and $\mathbf{E}$ is electric field.